

Regularized Laplacian Zero Crossings as Optimal Edge Integrators

R. KIMMEL A.M. BRUCKSTEIN
Department of Computer Science
Technion–Israel Institute of Technology
Technion City, Haifa 32000, Israel

Abstract

We view the fundamental edge integration problem for object segmentation in a geometric variational framework. First we show that the classical zero-crossings of the image Laplacian edge detector as suggested by Marr and Hildreth, inherently provides optimal edge-integration with regard to a very natural geometric functional. This functional accumulates the inner product between the normal to the edge and the gray level image-gradient along the edge. We use this observation to derive new and highly accurate active contours based on this functional and regularized by previously proposed geodesic active contour geometric variational models.

1. Introduction

Edge integration for segmentation is an old, yet still very active area of research in low-level image analysis. Text-books in computer vision treat edge detection and edge integration as separate topics, the first being considered one of labelling edges in the image to be followed by a process of integrating the local “edges” into meaningful curves. In fact one may view basic edge detection as a process of estimating the gradient of the image, i.e. computing at each pixel (x, y) the values $u(x, y)$ and $v(x, y)$ by using the values of $I(x, y)$ over a neighborhood $\mathcal{N}(x, y)$ of (x, y) and designating as edges the places where the length of the gradient vector estimate $[u, v] = (\nabla I)$ exceeds some threshold value.

The more advanced edge detectors such as those proposed by Marr and Hildreth [8] attempt to locate points or curves defined by local maxima of the image gradient. The Marr Hildreth proposal for edge detection yields curves that delineate the zero crossing of the Laplacian operator applied to a smoothed version of the image input. The smoothing proposed is via a Gaussian convolution operator and its width is a parameter that can be varied providing the opportunity to do scale space processing and “vertical” integration on the zero-crossing curves.

In this paper we propose to regard the edge detection and integration process as a way to determine curves in the

image plane that pass through points where the gradient is high and whose direction best corresponds to the local edge direction predicted by the estimated gradient.

Indeed, if we somehow estimate the gradient field $[u(x, y), v(x, y)]$ based on considering $I(x, y)$ for each pixel (x, y) over some neighborhood $\mathcal{N}_\sigma(x, y)$, where σ is a size parameter, we shall have at each point a value, given by the intensity of the gradient $(u^2(x, y) + v^2(x, y))^{\frac{1}{2}}$, that tells us how likely an edge is at this point and, if an edge exists, its likely direction will be perpendicular to the vector $[u(x, y), v(x, y)]$. It is therefore natural to look for curves in the image plane, $C(s) = [x(s), y(s)]$, that pass through points with high intensity gradients with tangents agreeing as much as possible to the edge directions there. Thus we are led to consider the following functional, evaluating the quality of $C(s)$ as an edge-curve candidate, $\psi_\rho(C(s)) =$

$$= \int_0^L \rho \left([u(C(s)), v(C(s))] \cdot \begin{bmatrix} 0 & 1 \\ -1 & 0 \end{bmatrix} \left[\frac{dC(s)}{ds} \right]^T \right) ds$$

where $\rho(\cdot)$ is some monotonically increasing function. Here, the inner product of $\nabla I = [u, v]$ with the normal to $C(s)$, given by $\vec{n}(s) = \begin{bmatrix} 0 & 1 \\ -1 & 0 \end{bmatrix} \left[\frac{dC(s)}{ds} \right]^T$, where $C(s)$ is an arclength parameterized curve, is a measure of how well $C(s)$ is locally tracking an edge. Indeed we want $C(s)$ to pass at high gradient locations in the edge direction, and hence the inner product of its normal with the estimated gradient of I should be high, indicating both alignment and considerable change in image intensity there. This inner product will also be proportional to the gradient magnitude, since

$$[u(C(s)), v(C(s))] \begin{bmatrix} 0 & 1 \\ -1 & 0 \end{bmatrix} \left[\frac{dC}{ds} \right]^T = |\nabla I| \cdot \cos(\theta),$$

where θ is the angle between the outward pointing normal \vec{n} to $C(s)$ and the gradient direction.

The functionals ψ_ρ measure how well an arclength parameterized curve of length L approximates an edge in the image plane. Our task, of course is to determine several most probable edge curves in the image plane. We shall do so by determining curves that locally maximize these functionals.

Suppose first that we are considering closed contours $C(s)$, and that $\rho(\alpha) = \alpha$. Then, we have that

$$\psi(C(s)) = \oint_{C(s)} \left(u(C(s)) \frac{d}{ds} y(s) - v(C(s)) \frac{d}{ds} x(s) \right) ds,$$

and Green's theorem yields

$$\psi(C(s)) = \iint_{\Omega_C} \left(\frac{\partial}{\partial y} v(x, y) + \frac{\partial}{\partial x} u(x, y) \right) dx dy,$$

where Ω_C is the region inside $C(s)$. But, recalling that $v(x, y)$ is an estimate of $\frac{\partial}{\partial y} I(x, y)$ and $u(x, y)$ an estimate of $\frac{\partial}{\partial x} I(x, y)$ we have

$$\begin{aligned} \psi(C(s)) &\cong \iint_{\Omega_C} \left(\frac{\partial^2}{\partial x^2} I(x, y) + \frac{\partial^2}{\partial y^2} I(x, y) \right) dx dy \\ &\cong \iint_{\Omega_C} (\Delta I(x, y)) dx dy. \end{aligned}$$

Therefore, the functional that we want to maximize is the integrated Laplacian over the area enclosed by $C(s)$. This means that if we have an area where the Laplacian is positive $\psi(C(s))$ should expand from within this area to the places where $\Delta I(x, y)$ becomes zero and subsequently changes sign. This shows that optimal edge-curves in the sense of maximizing $\psi(C(s))$ are the zero crossings of the Laplacian. If we initialize $C(s)$ as a small circular ‘bubble’ at a place where $\Delta I(x, y)$ is positive and then let $C(s)$ evolve according to a rule that implements a gradient descent in conjunction with the functional $\psi(C(s))$, i.e. we implement

$$\frac{d}{dt} C(s, t) = \frac{\delta \psi(C(s, t))}{\delta C},$$

the curve $C(s, t)$ will expand in time t to the nearest zero-crossing curve of the input image Laplacian.

Therefore, we have obtained a beautiful interpretation of the classical Marr-Hildreth edge detection method [8]. The zero-crossings of the Laplacian are curves that best integrate the edges, in the sense of our functional $\psi_\rho(C(s))$ with $\rho(\alpha) = \alpha$, if we wish to do so based on gradients estimated for the (smoothed) input image $I(x, y)$. While this fact is pedagogically very pleasing, it does not alleviate the notorious over sensitivity properties of this edge-detector which in noisy images yields lots of false edge curves. However, we shall show here that this insight provides the basis for a new and practical active contour process which enhances and improves upon the previously designed such methods for image segmentation.

We next present the full derivation of the variational results leading to the new edge integration processes and then show the performance of the resulting algorithms.

2. Closed Active Contours: Derivation

Motivated by the classical ‘snakes’ [4], geometric active contours [5, 1, 6], and finally the ‘geodesic active contours’ that were shown in [2] to be related to the ‘snakes’, we search for simple parametric curves in the plane that map their arclength interval $[0, L]$ to the plane, such that $C : [0, L] \rightarrow \mathbb{R}^2$, or in an explicit parametric form $C(s) = [x(s), y(s)]$. Here s is the arclength parameter, and we have the relation between the arclength s and a general arbitrary parameterization p , given by

$$ds = \sqrt{\left(\frac{dx(p)}{dp} \right)^2 + \left(\frac{dy(p)}{dp} \right)^2} dp = |C_p| dp.$$

We define, as usual, \vec{n} , κ , and \vec{t} to be the unit normal, the curvature, and the tangent of the curve C . We have that $\kappa \vec{n} = C_{ss}$, and $\vec{t} = C_s = C_p / |C_p|$. As described in the introduction, consider the geometric functional

$$\psi_\rho(C) = \int_0^L \rho(\langle \vec{V}, \vec{n} \rangle) ds.$$

This is an integration along the curve C of a function ρ defined in terms of a vector field $\vec{V} = [u(x, y), v(x, y)]$, where for example we can take $\vec{V} = \nabla I(x, y) = [I_x, I_y]$ as the gray level image gradient. Our goal is to find curves C that minimize the above geometric functional.

In a general parametric form, we have the following re-parameterization invariant measure

$$\psi_\rho(C) = \int_0^1 \rho(\langle \vec{V}, \vec{n} \rangle) |C_p| dp.$$

Define, $\alpha \equiv \langle \vec{V}, \vec{n} \rangle$. The Euler Lagrange (EL) equations $\delta \psi_\rho(C) / \delta C = 0$ should hold along the extremum curves, and for a closed curve these equations are

$$\frac{\delta \psi_\rho(C)}{\delta C} = \left(\frac{\frac{\partial}{\partial x} - \frac{d}{dp} \frac{\partial}{\partial x_p}}{\frac{\partial}{\partial y} - \frac{d}{dp} \frac{\partial}{\partial y_p}} \right) \rho(\alpha) |C_p|,$$

or in a more compact form

$$\frac{\delta \psi_\rho(C)}{\delta C} = \left(\frac{\partial}{\partial C} - \frac{d}{dp} \frac{\partial}{\partial C_p} \right) \rho(\alpha) |C_p|,$$

where we use the shorthand notation $\partial / \partial C = [\partial / \partial x, \partial / \partial y]^T$ and $\partial / \partial C_p = [\partial / \partial x_p, \partial / \partial y_p]^T$. In case of an open curve, one must also consider the end points and add additional constraints to determine their optimal locations.

Before we work out the general $\rho(\alpha)$ case let us return to the simple example discussed in the introduction, where $\rho(\alpha) = \alpha$. In this case we have that

$$\psi(C) = \int_0^1 \langle \vec{V}, \vec{n} \rangle |C_p| dp$$

$$\begin{aligned}
&= \oint_0^1 \left\langle \vec{V}, \frac{[-y_p, x_p]}{|C_p|} \right\rangle |C_p| dp \\
&= \oint_0^1 (-y_p u + x_p v) dp.
\end{aligned}$$

The EL equation for the x part is given by

$$\begin{aligned}
\frac{\delta\psi}{\delta x} &= \left(\frac{\partial}{\partial x} - \frac{d}{dp} \frac{\partial}{\partial x_p} \right) (-y_p u + x_p v) \\
&= -y_p u_x + x_p v_x - \frac{d}{dp} v \\
&= -y_p u_x + x_p v_x - v_x x_p - v_y y_p \\
&= -y_p (u_x + v_y) = -y_p \operatorname{div}(\vec{V}).
\end{aligned}$$

In a similar way, the y part of the EL equations is given by

$$\begin{aligned}
\frac{\delta\psi}{\delta y} &= \left(\frac{\partial}{\partial y} - \frac{d}{dp} \frac{\partial}{\partial y_p} \right) (-y_p u + x_p v) \\
&= -y_p u_y + x_p v_y + \frac{d}{dp} u \\
&= -y_p u_y + x_p v_y + u_x x_p + u_y y_p \\
&= x_p (u_x + v_y) = x_p \operatorname{div}(\vec{V}).
\end{aligned}$$

Since the EL equations are derived with respect to a geometric measure, we can use the freedom of reparameterization for the curve C , divide by $|C_p|$, and obtain the ‘‘geometric EL equation:’’ $\delta\psi/\delta C = \operatorname{div}(\vec{V})\vec{n}$, and for $\vec{V} = \nabla I(x, y)$ we have $\delta\psi/\delta C = \Delta I \vec{n}$, where $\Delta I \equiv I_{xx} + I_{yy}$ is the usual Laplacian operator. It is obvious from this that the geometric EL condition is satisfied along the zero crossing curves of the image Laplacian, which as described above explains the Marr-Hildreth [8, 7] edge detector from a global-variational point of view. Below, we shall extract further insights and segmentation schemes from this observation. We note that heuristic non-variational flows on vector fields were presented in [14, 11]. In a recent related result, introduced by Vasilevskiy and Siddiqi [13], alignment with a vector field is used as a minimization criteria for segmentation of complicated closed thin structures in 3D medical images.

As a second example we consider $\rho(\alpha) = |\alpha| = \sqrt{\alpha^2}$. The EL is given by

$$\begin{aligned}
\frac{\delta\psi}{\delta C} &= \frac{\langle \vec{V}, \vec{n} \rangle}{|\langle \vec{V}, \vec{n} \rangle|} \operatorname{div}(\vec{V})\vec{n} \\
&= \operatorname{sign}(\langle \vec{V}, \vec{n} \rangle) \operatorname{div}(\vec{V})\vec{n},
\end{aligned}$$

and for $\vec{V} = \nabla I$ we have $\delta\psi/\delta C = \operatorname{sign}(\langle \nabla I, \vec{n} \rangle) \Delta I \vec{n}$. The new term $\operatorname{sign}(\langle \nabla I, \vec{n} \rangle)$, allows the model to automatically handle changing contrasts between the objects and the background. For example, it handles equally well an image of dark objects on bright background and the negative of this image.

Now, we are ready to pursue the general case for $\rho(\alpha)$ in the functional $\psi_\rho(C)$ (where $\alpha = \langle \vec{V}, \vec{n} \rangle$). We shall use

often the following readily verified relationships,

$$\begin{aligned}
\frac{d}{dp} &= |C_p| \frac{d}{ds} & \frac{\partial |C_p|}{\partial C_p} &= \vec{t} \\
\frac{d\vec{n}}{ds} &= -\kappa \vec{t} & \frac{d\vec{t}}{ds} &= \kappa \vec{n} \\
\frac{d\rho(\alpha)}{ds} &= \rho' \alpha_s = \langle \nabla \rho, \vec{t} \rangle & & \\
\frac{d\alpha}{ds} &= \langle \vec{V}_s, \vec{n} \rangle + \langle \vec{V}, \vec{n}_s \rangle = \langle \vec{V}_s, \vec{n} \rangle - \kappa \langle \vec{V}, \vec{t} \rangle \\
\frac{\partial \alpha}{\partial C_p} &= -|C_p|^{-1} \langle \vec{V}, \vec{t} \rangle \vec{n}, & &
\end{aligned}$$

and that

$$\left(\frac{\partial}{\partial C} - \frac{d}{dp} \frac{\partial}{\partial C_p} \right) (\alpha |C_p|) = |C_p| \operatorname{div}(\vec{V})\vec{n}.$$

Using these relations we have

$$\begin{aligned}
\frac{\delta\psi_\rho(C)}{\delta C} &= \left(\frac{\partial}{\partial C} - \frac{d}{dp} \frac{\partial}{\partial C_p} \right) \rho(\alpha) |C_p| = \\
&= \rho' \alpha_C |C_p| - \frac{d}{dp} (\rho' \alpha_{C_p} |C_p| + \rho \vec{t}) \\
&= \rho' \alpha_C |C_p| - \frac{d}{dp} (\rho' \alpha_{C_p} |C_p| + \rho' \alpha \vec{t}) - \frac{d}{dp} (-\rho' \alpha \vec{t} + \rho \vec{t}) \\
&= \rho' \alpha_C |C_p| - \rho' \frac{d}{dp} (\alpha_{C_p} |C_p| + \alpha \vec{t}) \\
&\quad - \rho'' \alpha_p (\alpha_{C_p} |C_p| + \alpha \vec{t}) - \frac{d}{dp} (-\rho' \alpha \vec{t} + \rho \vec{t}) \\
&= \rho' |C_p| \operatorname{div}(\vec{V})\vec{n} - \rho'' |C_p| \alpha_s (\langle \vec{V}, \vec{t} \rangle \vec{n} + \alpha \vec{t}) \\
&\quad - |C_p| \frac{d}{ds} (-\rho' \alpha \vec{t} + \rho \vec{t}) \\
&= |C_p| \left(-\rho \kappa + \rho' (\operatorname{div}(\vec{V}) + \langle \vec{V}, \vec{n} \rangle \kappa) + \rho'' (\langle \vec{V}_s, \vec{n} \rangle \langle \vec{V}, \vec{t} \rangle \right. \\
&\quad \left. - \kappa \langle \vec{V}, \vec{t} \rangle^2) \right) \vec{n} + \text{some additional tangential components.}
\end{aligned}$$

Here we used the shorthand notations $\alpha_C = \nabla \alpha = [\alpha_x, \alpha_y]$, and $\alpha_{C_p} = \nabla_{C_p} \alpha$.

Level Set Formulation: In order to determine optimal curves in the plane, we need to solve numerically the EL equations. Here we shall follow the ‘‘geodesic active contour philosophy,’’ see [2], and design a curve evolution rule that is given by $C_t = \frac{\delta\psi_\rho(C)}{\delta C}$. This is a gradient descent rule with respect to the chosen cost functional, and in this flow one can consider only the normal components of $\delta\psi_\rho(C)/\delta C$, since tangential components have no effect on the geometry of the propagating curve. Next, we can embed the curve in a higher dimensional $\phi(x, y)$ function, which implicitly represents the curve C as a zero set, i.e., $C = \{[x, y] : \phi(x, y) = 0\}$. In this way, the well known Osher-Sethian [9, 12] level-set method can be employed to implement the propagation.

Given the curve evolution equation $C_t = \gamma \vec{n}$, its implicit level set evolution equation reads $\phi_t = \gamma |\nabla \phi|$. The equivalence of these two evolutions can be easily verified using the chain rule and the relation $\vec{n} = \nabla \phi / |\nabla \phi|$,

$$\phi_t = \langle \nabla \phi, C_t \rangle = \langle \nabla \phi, \gamma \vec{n} \rangle = \gamma \left\langle \nabla \phi, \frac{\nabla \phi}{|\nabla \phi|} \right\rangle = \gamma |\nabla \phi|.$$

We readily have that $\vec{t} = \frac{\nabla\phi}{|\nabla\phi|} = \frac{[-\phi_y, \phi_x]}{|\nabla\phi|}$, $\kappa = \text{div}\left(\frac{\nabla\phi}{|\nabla\phi|}\right)$, $\vec{V}_s = [u_s, v_s] = [\langle \nabla u, \vec{t} \rangle, \langle \nabla v, \vec{t} \rangle]$, and $\text{sign}(\langle \vec{V}, \vec{n} \rangle) = \text{sign}(\langle \vec{V}, \nabla\phi \rangle)$. Thereby, the explicit curve evolution as a gradient descent flow for $\rho(\alpha) = |\alpha|$ is given by

$$C_t = \text{sign}(\langle \vec{V}, \vec{n} \rangle) \Delta I \vec{n},$$

for which the implicit level set evolution is given by

$$\phi_t = \text{sign}(\langle \vec{V}, \nabla\phi \rangle) \Delta I |\nabla\phi|.$$

3. Open Active Contours

Fua and Leclerc in [3], were first to propose a geometric model for motion of open curves in the image to optimize an “edge” finding functional. We shall first describe the Fua-Leclerc functional and then replace the “geodesic active contour” part of it with our new edge integration quality measure. Let $L(C) = \int_0^1 |C_p| dp$, be the arlength of an open curve $C(p)$. Adding the variation $\eta(p)$ to the curve, such that $\tilde{C}(p) = C(p) + \epsilon\eta(p)$, differentiating w.r.t. ϵ , and letting ϵ go to zero, yields

$$L'(C) = - \int_0^L \kappa \vec{n} \eta ds + \eta(L) \vec{t}(L) - \eta(0) \vec{t}(0),$$

where s is the arlength parameter. Also, following Fua and Leclerc, consider $L_g(C) = \int_0^L g(C(s)) ds$, where g is some suitably defined “edge indicator” function, for example $g(x, y) = 1/(|\nabla I|^2 + 1)$. The first variation of $L_g(C)$ can be easily shown to be given by

$$L'_g(C) = \int_0^L (\langle \nabla g, \vec{n} \rangle - \kappa g) \vec{n} \eta ds + \eta(L) g(C(L)) \vec{t}(L) - \eta(0) g(C(0)) \vec{t}(0).$$

The Fua-Leclerc functional is defined as $\psi_g(C) = \frac{L_g(C)}{L(C)}$. Computing the first variation, we have that $\frac{\delta\psi_g}{\delta C} = \frac{LL'_g - L'L_g}{L^2} = 0$, should hold for any η . Therefore, the following conditions must be satisfied, $LL'_g = L'L_g$, or explicitly,

$$\begin{aligned} L \cdot \left(\int_0^L (\langle \nabla g, \vec{n} \rangle - \kappa g) \vec{n} \eta ds + \eta(L) g(C(L)) \vec{t}(L) - \eta(0) g(C(0)) \vec{t}(0) \right) \\ = L_g \cdot \left(\int_0^L -\kappa \vec{n} \eta ds + \eta(L) \vec{t}(L) - \eta(0) \vec{t}(0) \right). \end{aligned}$$

Thus, we should verify the following necessary conditions for a local extremum to hold for any η ,

$$\begin{aligned} \int_0^L (L(\langle \nabla g, \vec{n} \rangle - \kappa g) + L_g \kappa) \vec{n} \eta ds &= 0 \\ L\eta(L)g(C(L))\vec{t}(L) &= L_g\eta(L)\vec{t}(L) \\ L\eta(0)g(C(0))\vec{t}(0) &= L_g\eta(0)\vec{t}(0). \end{aligned}$$

Therefore, the geometric conditions that must be met along the curve is $\left(\left(\frac{L_g}{L} - g \right) \kappa + \langle \nabla g, \vec{n} \rangle \right) \vec{n} = 0$, and at its end points $g(C(0)) = \frac{L_g}{L}$, and $g(C(L)) = \frac{L_g}{L}$. We can use these conditions to guide a gradient descent process for an active contour evolution toward the local minimum of the Fua-Leclerc functional. To do that we apply the following evolution equation along the curve and at its end points,

$$C_t = \left(\kappa g - \langle \nabla g, \vec{n} \rangle - \frac{L_g}{L} \kappa \right) \vec{n}.$$

The first two terms depict the geodesic active contour ([2]) model, while the third term directs the curve to gain length by applying the inverse geometric heat equation at points where $g(C(s)) < L_g/L$. We still need to design the motion of the end points. Consider the end point $C(L)$. The curve should reduce its length if $g(C(L)) > L_g/L$, in which case the end point should move along the tangent $-\vec{t}(L)$. Hence, for example, we can use the following evolution rules at the end points:

$$\begin{aligned} C_t(0) &= (Lg(C(0)) - L_g) \vec{t}(0) \\ C_t(L) &= (L_g - Lg(C(L))) \vec{t}(L). \end{aligned}$$

Optimal Edge Integration: We propose to use our measure, $L_\rho = \int \rho(\alpha) ds$ instead of L_g , in the Fua-Leclerc functional. Here we compute the evolution equations that propagate the open curve C towards a maximum of the functional $\psi_\rho(C) = \frac{L_\rho}{L}$. Therefore, we are searching for $\arg_C \max \psi_\rho(C)$. The quantity L in this *maximization* process, penalizes the length of the curve, i.e. it plays a role opposite from its role in the *minimization* of the Fua-Leclerc functional.

We now use the $\delta\psi_\rho/\delta C$ expression developed in the previous sections for the general $\rho(\langle \vec{V}, \vec{n} \rangle)$ closed curve case. We have that

$$L'_\rho(C) = \int_0^L \eta \frac{\delta\psi_\rho}{\delta C} ds + \eta \left(\rho \vec{t} - \rho' \langle \vec{V}, \vec{t} \rangle \vec{n} \right) \Big|_0^L.$$

Using these conditions in the Fua-Leclerc formulae yield along the curve, $L \frac{\delta\psi_\rho}{\delta C} + L_\rho \kappa \vec{n} = 0$, and $L(\rho \vec{t} - \rho' \langle \vec{V}, \vec{t} \rangle \vec{n}) = L_\rho \vec{t}$, at the end points $C(L)$ and $C(0)$. For $\rho(\alpha) = |\alpha|$, the gradient descent flow of the curve is given by

$$\begin{aligned} C_t &= \text{sign}(\langle \nabla I, \vec{n} \rangle) \Delta I \vec{n} + \frac{L_\rho}{L} \kappa \vec{n} \\ C_t(0) &= (L_\rho - L_\rho) \vec{t} - \rho' \langle \vec{V}, \vec{t} \rangle \vec{n} \\ C_t(L) &= (L_\rho - L_\rho) \vec{t} + \rho' \langle \vec{V}, \vec{t} \rangle \vec{n}. \end{aligned}$$

A Simpler Optimal Edge Integration: Functionals that involve ratio of two integral measures, like the Fua-Leclerc functional, require integration along the contours for a

proper gradient descent flow. Integral parts are present in the EL equations which require computationally intensive global integration procedures for the computation of the proper flow. Recall however that our goal is to maximize $\psi_\rho(C)$ on one hand, that leads to long curves, while also penalizing the length of the curve on the other hand. We shall therefore consider the following alternative functional that would also realize these goals, $\psi_\rho(C) = L_\rho - L$. The EL equations in this case are given by $0 = \frac{\delta\psi_\rho(C)}{\delta C} + \kappa\vec{n}$, along the curve, and $0 = (\rho - 1)\vec{t} - \rho'\langle\vec{V}, \vec{t}\rangle\vec{n}$, at the end points. The motivation for the tangential term at the end point is obvious, it either extends or shrinks the curve. The normal term pulls it from running parallel to the vector field and directs the end point towards the center of the edge (where ρ' should be zero). These two components define the motion at the end points. For $\rho(\alpha) = |\alpha|$ and $\vec{V} = \nabla I$ we have

$$\begin{aligned} C_t &= \text{sign}(\langle\nabla I, \vec{n}\rangle)\Delta I\vec{n} + \kappa\vec{n} \\ C_t(0) &= (|\langle\nabla I, \vec{n}\rangle| - 1)\vec{t} - \text{sign}(\langle\nabla I, \vec{n}\rangle)\langle\nabla I, \vec{t}\rangle\vec{n} \\ C_t(L) &= (1 - |\langle\nabla I, \vec{n}\rangle|)\vec{t} + \text{sign}(\langle\nabla I, \vec{n}\rangle)\langle\nabla I, \vec{t}\rangle\vec{n}. \end{aligned}$$

4. Simulation Results

We tested the edge integration methods discussed in this paper on two simple examples. The first presented segmentation examples shown are not typical for active contours and could be easily processed with less sophisticated methods. However, they capture the difficulties of the existing active contour models and therefore are useful for comparison of the different methods.

In the "closed contour" cases we started from the image frame as the initial contour, and applied a multi-resolution coarse to fine procedure, as in [10], to speed up the segmentation process.

Figure 1 shows the advantage of the Laplacian model in cases where only the gradient is affected, the Laplacian being invariant to an additive intensity plane, as well as in cases where the Laplacian is also changed by a constant when a parabola was added to the intensity surface. Figure 2 clearly exhibit the segmentation advantages of the Laplacian active curve model as a core with the geodesic active term as a regularization. We here used the functional

$$\psi(C) = \oint_C \rho(\alpha)ds - \beta \oint_C g_1(C(s))ds - \lambda \int_{\Omega_C} g_2(x, y)dx dy,$$

where β and λ are small positive constants, $\rho(\alpha) = |\alpha|$, and $\alpha = \langle\nabla I, \vec{n}\rangle$. $g_i, i = 1, 2$ are edge indicator functions with lower values along the edges. In this case, the gradient descent flow for maximizing $\psi(C)$ is given by

$$C_t = (\text{sign}(\langle\nabla I, \vec{n}\rangle)\Delta I + \beta(g_1\kappa - \langle\nabla g_1, \vec{n}\rangle) - \lambda g_2)\vec{n}.$$

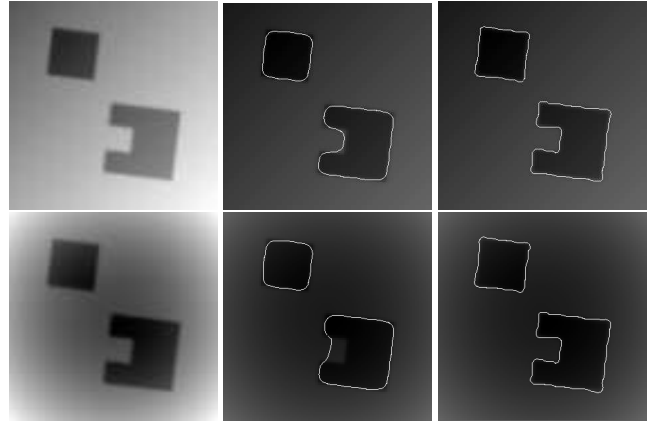


Figure 1: Synthetic images with a tilted intensity plane (top) and a parabola intensity surface (bottom) added to the original image. Middle: GAC results. Left: Laplacian model results.

The level set formulation for this flow is

$$\phi_t = \left(\text{sign}(\langle\nabla I, \nabla\phi\rangle)\Delta I + \beta \text{div} \left(g_1 \frac{\nabla\phi}{|\nabla\phi|} \right) - \lambda g_2 \right) |\nabla\phi|.$$

Next, we applied our open contour model for edge integration on similar images, but here we started with short contour segments that expanded and locked onto boundaries, if such existed in the vicinity of the initialized contours. If no boundaries are detected locally, the contour segments shrink and eventually disappear. The numerical implementation for the open contour case is an explicit "marker-points" based model which was easier to program in this case. At each iteration the marker-points are redistributed along the contour to form equi-distant numerical representations of the contour. A simple monitoring procedure, removes a marker point when successive marker points get too close to one another, and adds a new marker point in the middle of two successive marker points when the distance between them gets larger than a given threshold. The examples show how initial segments expand and deform until they lock onto the boundaries of rather complex shapes. See 3.

5. Conclusions

In this paper we proposed to incorporate the directional information that is generally ignored when designing edge integration methods in a variational framework. Simulations that were performed with the newly defined edge integration processes amply demonstrated their excellent performance as compared to the best existing edge integration methods. Our extended active contour models are just a few examples of the many possible combinations of geometric mea-

tures. Other functionals that could be considered to either open or closed curves are $L_\rho - L_g$, or $\int \rho(\alpha)q(|\nabla I|)ds$, for an edge indicator function like $q = 1 - g(|\nabla I|)$ or $q(|\nabla I|) = \sqrt{|\nabla I|^2 + 1}$. For closed curves, the ψ_ρ part is most effective when the curve is close to its final location, therefore, the functional $\oint [\rho(\alpha)(1-g) - g]ds$ could also be considered.

Acknowledgments

We thank Evgeni Krimer and Roman Barsky for implementing and testing the open active contours models.

References

- [1] V. Caselles, F. Catte, T. Coll, and F. Dibos. A geometric model for active contours. *Numerische Mathematik*, 66:1–31, 1993.
- [2] V. Caselles, R. Kimmel, and G. Sapiro. Geodesic active contours. *IJCV*, 22(1):61–79, 1997.
- [3] P. Fua and Y. G. Leclerc. Model driven edge detection. *Machine Vision and Applications*, 3:45–56, 1990.
- [4] M. Kass, A. Witkin, and D. Terzopoulos. Snakes: Active contour models. *International Journal of Computer Vision*, 1:321–331, 1988.
- [5] R. Malladi, J. Sethian, and B. C. Vemuri. A topology-independent shape modeling scheme. In *SPIE's Geometric Methods in Computer Vision II*, volume SPIE 2031, pages 246–255, July 1993.
- [6] R. Malladi, J. Sethian, and B. C. Vemuri. Shape modeling with front propagation: A level set approach. *IEEE Trans. on PAMI*, 17:158–175, 1995.
- [7] D. Marr. *Vision*. Freeman, San Francisco, 1982.
- [8] D. Marr and E. Hildreth. Theory of edge detection. *Proc. of the Royal Society London B*, 207:187–217, 1980.
- [9] S. J. Osher and J. Sethian. Fronts propagating with curvature dependent speed: Algorithms based on Hamilton-Jacobi formulations. *J. of Comp. Phys.*, 79:12–49, 1988.
- [10] N. Paragios and R. Deriche. Geodesic active contours and level sets for the detection and tracking of moving objects. *IEEE Trans. on PAMI*, 22(3):266–280, 2000.
- [11] N. K. Paragios, O. Mellina-Gotardo, and V. Ramesh. Gradient vector flow fast geodesic active contours. In *Proceedings ICCV'95*, Vancouver, Canada, July 2001.
- [12] J. Sethian. *Level Set Methods: Evolving Interfaces in Geometry, Fluid Mechanics, Computer Vision and Materials Sciences*. Cambridge Univ. Press, 1996.
- [13] A. Vasilevskiy and K. Siddiqi. Flux maximizing geometric flows. In *Proceedings ICCV'95*, Vancouver, Canada, July 2001.
- [14] C. Xu and J. Prince. Snakes, shapes, and gradient vector flow. *IEEE Trans. IP*, 7(3):359–369, 1998.

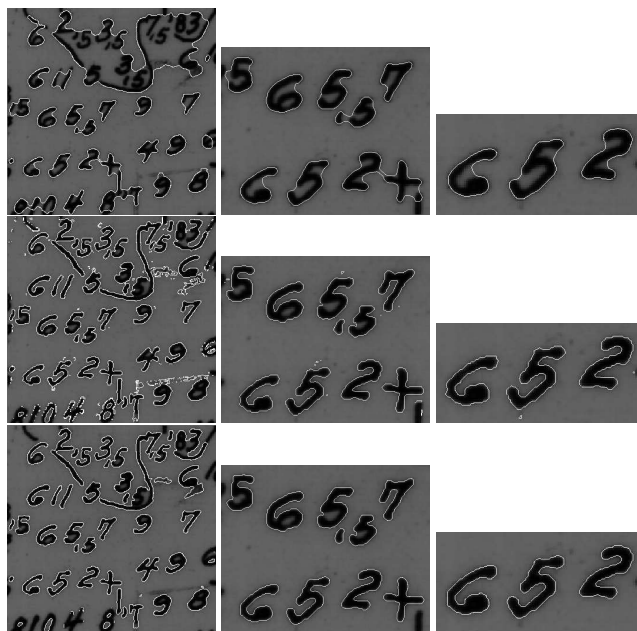


Figure 2: Top: Geodesic active contour results. Middle: Laplacian active contours. Bottom: Using the geodesic active contours as a regularization for the Laplacian active contour.

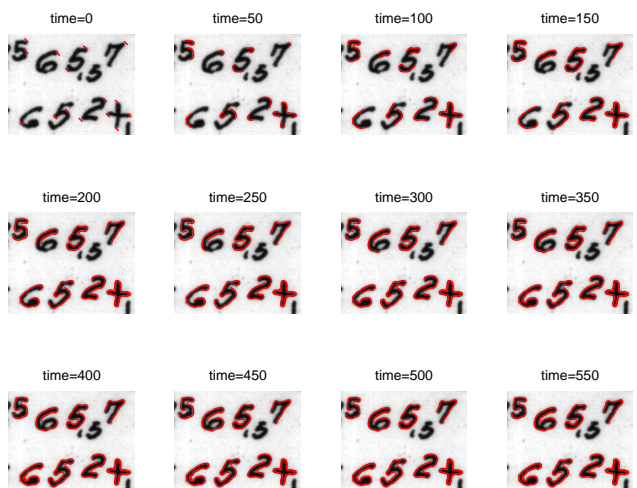


Figure 3: Open geometric Laplacian active contours: The small curves (top left frame) extend along the boundaries and capture most of the outer contours of the symbols.